A Design Procedure for a PM Machine with Extended Field Weakening Capability

Juan A. Tapia, *Student Member* Franco Leonardi, *Member* Thomas A. Lipo, *Fellow*

***Abstract*— A design procedure for the Consequent Pole Permanent Magnet (CPPM) machine is presented. Due its double excitation nature (PM and field winding) and inherent three-dimensional flux distribution an apropriate set of equations must be derived to model its magnetic structure. For practical operating conditions, radial, axial and tangential flux component are present. Therefore a convenient representation of the magnetic sources and their magnetic paths are necessary. For this purpose, a simplified reluctance-based equivalent circuit for 2-poles is developed to capture the main features of the machine. Approximated expressions for the airgap flux and the airgap flux density are derived. In these expressions the constant contribution of the PM and the variable flux provided by the field winding are taken into account. In addition, a formulation to calculate AC and DC slot geometry, copper and iron losses estimation and output power are developed. Finally, an optimization procedure is outlined based on maximum material utilization under current and magnetic loading constraints.**

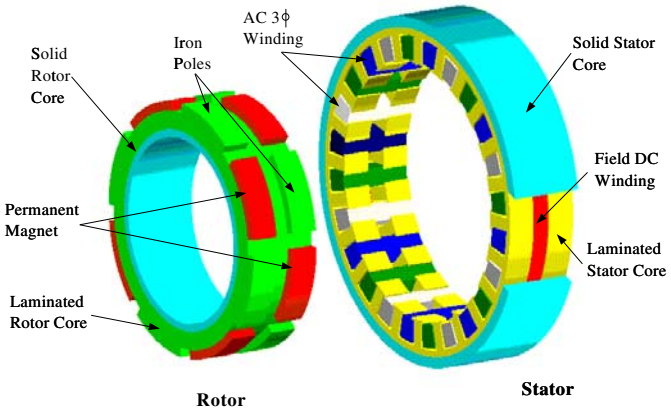

Fig. 1. Structure of the CPPM machine

I. Introduction

It has been shown that the Consequent Pole Permanent Magnet (CPPM) machine has atractive features for variable speed AC drives applications [1]. Due to the feature of double excitation (PM and field winding) a wide range of airgap flux can be achieved with a modest amount of field MMF. In addition, there does not exist a demagnetization risk for the magnets. Control action is made over soft iron poles. Slip rings, brushes or other mobile contact are not required to transfer energy to the field winding because it is located in the stator.

The operation of the CPPM machine involves a three-dimensional (3D) flux distribution which increases the analytical complexity. Modern 3D finite element analysis software is clearly suitable to predict the performance of this type of structure. However, excessive memory and processing time greatly slow the design task [2], and the software does not yield convenient expressions between variables and parameter to find functional dependence.

In this paper a simplified reluctance equivalent circuit for design purposes is developed for the CPPM machine. This circuit captures the sense of the machine operation and allows one determination of the functional dependence between the design variables. In particular, approximate expressions for the airgap flux and the airgap flux density are derived. In these expressions the constant contribution of the PM and the variable flux provided by the field winding are taken into account, considering separated equivalent circuits. In addition, formulations to calculate AC and DC slot geometry, copper and iron losses estimation and output power are derived. Finally, an optimization procedure is outlined based on maximum material utilization under heat evacuation constraints.

Juan A. Tapia is with Dept. of Electrical Engineering University of Concepcion Casilla 160-C, Correo 3 Concepcion, CHILE

Franco Leonardi is with the Vehicle Electronic Systems Department Ford Research Laboratories Dearborn MI 48120 Ph./fax 313-390-6923

Thomas A. Lipo is with Dept. of Electrical and Computer Engineering University of Wisconsin-Madison 1415 Engineering Dr Madison WI 53706-1651 USA Tel:(608) 265-0727 Fax(608) 262-5559

II. Reluctance Equivalent Circuit

If saturation is neglected, the reluctance equivalent circuit for one pole pair can be obtained based on the CPPM machine structure (see figure 3). Most of the flux created by the PM crosses the airgap and flows into the stator, closing the loop through the stator core and the next consecutive magnet. Flux created by the field winding follows a low reluctance path closing the loop along to stator core and the adjoining iron pole. Also, leakage flux is present between PM and air, an PM and iron poles which reduce the mutual flux linkages [3].

Figure 2 shows a simplified 2-pole magnetic circuit for the CPPM machine. In order to take advantage of the magnetic circuit symmetry, half of each pole is considered. The reluctance equivalent circuit for the magnetic circuit is depicted in figure 3. This simplified equivalent circuit considers both types of machine excitation (PMs and field current), the spatial flux distribution in the machine as well as flux leakages.

A careful analysis of this circuit allows separation of the circuit for both PM and field flux. Flux produced by the field current (marked by the small dashed line) flows through stator and rotor core, and iron poles. Neglecting the soft iron reluctance, an equivalent circuit for this flux can be drawn as shown in figure 3. On the other hand, PM flux (marked by the larger

0-7803-7420-7/02/$17.00 (C) 2002 IEEE

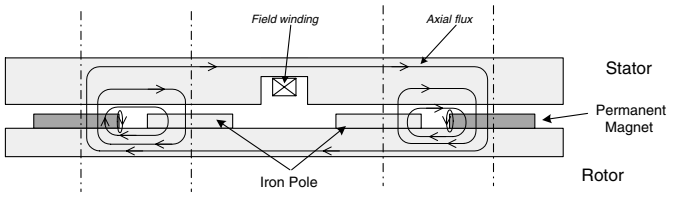

Fig. 2. 2-pole extended magnetic circuit of the CPPM machine

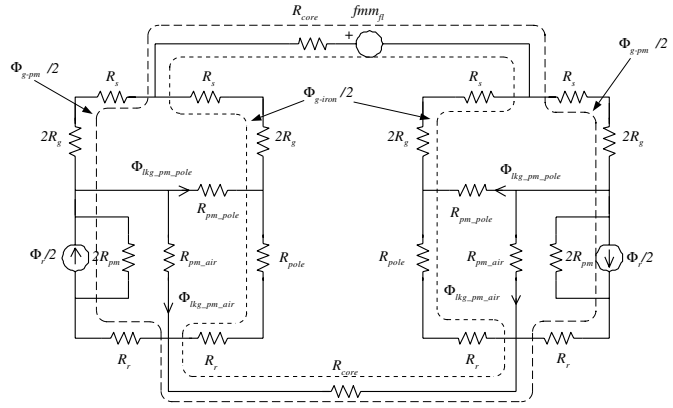

Fig. 3. Reluctance based equivalent circuit of figure 2.

dashed line) flows primarily in the stator and rotor core and in the magnet themselves.

III. Flux Distribution in the CPPM machine

When current is injected into the field winding (in either positive or negative directions), flux in the iron pole section changes linearly if the iron saturation is neglected. As a result the flux associated with the permanent magnet is invariant. The combination of these two fluxes results in the total airgap flux. This resultant can be either the summation or subtraction of the each component, depending upon the direction of the field current.

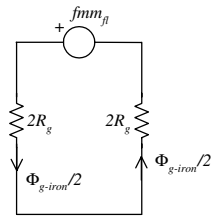

Fig. 4. Requivalent circuit for the field flux

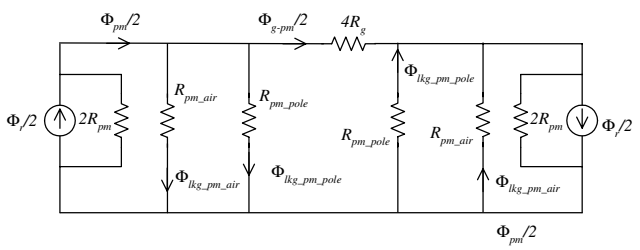

Fig. 5. Reluctance based equivalent circuit for the PM flux

A. Iron Section Component

¿From figure 4, it is a simple matter to calculate the iron component of the airgap flux as:

$$\Phi_{g-iron} = \frac{mmf_{fl}}{4R_g} \tag{1}$$

where mmf_{fl} are the Ampere-Turn of the field winding defined as

$$mmf_{fl} = N_{fl} I_{fl} \tag{2}$$

with N_{fl} and I_{fl} are the number of turns and the DC current of the field winding, respectively.

The flux density for the iron pole portion is calculated as:

$$B_{g-iron} = \frac{\Phi_{g-iron}}{\frac{A_g}{2}} \tag{3}$$

where A_g is the airgap area given by

$$A_g = D_{is} \frac{\pi}{p} l_{iron} \tag{4}$$

Using equations 1 and 4 , this expression becomes:

$$B_{g-iron} = K_{DC} \mu_o \frac{N_{fl} I_{fl}}{2g_e} \tag{5}$$

The factor K_{DC} considers the DC field current polarity, and its effect of the field flux in the airgap. $K_{DC} = +1$ when magnetizing effect of the field flux is present. If no DC field current is present, no-iron flux component exits and $K_{DC} = 0$. For the demagnetizing effect this factor assumes a value of -1.

According to eq. 5, the airgap flux density at the iron section is mainly determined by the field Ampere-Turns and by the airgap length.

B. PM Section Component

The PM flux component closes the loop following the path to the next PM pole. From figure 5

$$\Phi_{g-pm} = \frac{2R_{pm} \parallel R_{lg}}{2R_g + 2R_{pm} \parallel R_{lg}} \Phi_r \tag{6}$$

where "$\parallel$" denotes the reluctance parallel combination, and the R_{lg} is the combined leakage reluctance defined as:

$$R_{lg} = 2R_{pm-air} \parallel 2R_{pm-pole} \tag{7}$$

Developing the expression for the airgap flux in front of the PM section and the flux due to the remanence:

$$\Phi_{g-pm} = B_{g-pm} A_g \tag{8}$$

$$\Phi_r = B_r A_{pm} \tag{9}$$

where A_{pm} is the PM area given by

$$A_{pm} = \alpha_{pm} D_{is} \frac{\pi}{p} l_{pm} \tag{10}$$

therefore using eq. 8 and 9 in 6 , the flux density in front of the PM has the following expression

$$B_{g-pm} = \frac{2R_{pm} \parallel R_{lg}}{2R_g + 2R_{pm} \parallel R_{lg}} \frac{A_{pm}}{A_g} B_r \tag{11}$$

Introducing eqs. 4 and 10 the last expression becomes

$$B_{g-pm} = \frac{2R_{pm} \parallel R_{lg}}{2R_g + 2R_{pm} \parallel R_{lg}} \alpha_{pm} \frac{l_{pm}}{l_{iron}} B_r \tag{12}$$

The airgap flux density in the PM section, according to eq. 12, is mainly function of the PM magnetic parameters and the geometry of the magnet. In general, due to small value of airgap length with respect to the PM height and a nearly unity permeability of the magnet, the airgap length has only a minor influence on the flux density expression. Thus the magnet properties dominate over the other magnetic circuit parameters.

C. Airgap Flux and Flux Density

Total airgap flux is the summation of the PM and iron section calculated previously.

$$\Phi_g = \Phi_{g-iron} + \Phi_{g-pm} \tag{13}$$

Combining eqs. 1 and 6, airgap flux becomes:

$$\Phi_g = \frac{mmf_{fl}}{4R_g} + \frac{2R_{pm} \parallel R_{lg}}{2R_g + 2R_{pm} \parallel R_{lg}} \Phi_r \tag{14}$$

Airgap flux density is calculated as

$$B_g = \frac{\Phi_g}{A_g} \tag{15}$$

Decomposing airgap flux and airgap surface in their respective components:

$$B_g = \frac{\Phi_{g-iron} + \Phi_{g-pm}}{A_{g-iron} + A_{g-pm}} \tag{16}$$

Assuming, $A_{pm} = A_{iron}$

$$B_g = \frac{\Phi_{g-iron} + \Phi_{g-pm}}{2A_{pm}(or 2A_{iron})} \tag{17}$$

or

$$B_g = \frac{\Phi_{g-iron}}{2A_{iron}} + \frac{\Phi_{g-pm}}{2A_{pm}} \tag{18}$$

Therefore, in terms of the airgap flux density in each component is:

$$B_g = \frac{B_{g-iron}}{2} + \frac{B_{g-pm}}{2} \tag{19}$$

Introducing eq. 5 and 11 in the previous one, the airgap flux density becomes

$$B_g = K_{DC}\mu_o \frac{N_{fj} I_{fl}}{4g} + \frac{R_{pm} \parallel R_{lg}}{2R_g + 2R_{pm} \parallel R_{lg}} \alpha_{pm} \frac{l_{pm}}{l_{iron}} B_r \tag{20}$$

Eqs 14 and 20 are the per pole airgap flux and airgap flux density expression for the CPPM machine. Constant and variable components are represented in those equations. The variable one is function of the field Ampere-Turns and the constant term is defined by the PMs magnetic characteristics.

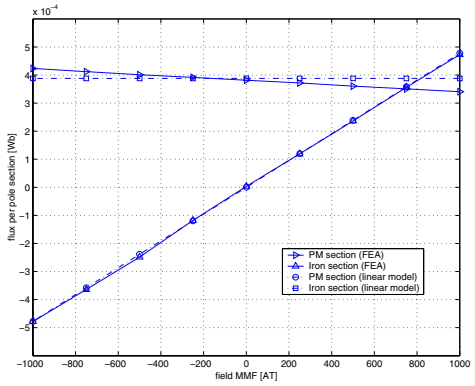

Fig. 6. Comparison with the linear model: eqs. 5 and 6 with 3D-FEA

D. Verification using Finite Element Analysis

Eqs. 5 and 6 have been calculated using a linear reluctance equivalent circuit. A verification of their exactness is made using 3D finite element analysis (FEA). Comparisons between the analytical model and FEA are depicted in figure 6. Both solutions predict, with only slight differences, the airgap flux component. Variation of the iron pole flux closely follows the expression obtained, eq. 5, in both magnitude and direction. The PM flux component, according to eq. 6, is a constant magnitude for any value of field Ampere-Turns. However, FEA shows that variation in this airgap components due to the iron flux component. It should be noted that cross coupling which is not considered for the analytical equation, is present due to the leakage flux.

IV. Losses in the CPPM machine

A. Conduction losses

1) DC field losses : Conduction losses in the DC field winding are calculated as:

$$P_{DC} = I_{fl}^2 R_{DC} \tag{21}$$

where R_{DC} is the resistance of the DC winding defined as:

$$R_{DC} = \rho_{cu} \frac{l_{fl-cond}}{A_{fl-cond}} \tag{22}$$

with $l_{fl-cond}$ and $A_{fl-cond}$ the length and conductor section area used in the DC field winding. Considering the mean line of the field winding slot, the conductor length can be expressed as:

$$l_{fl-cond} = N_{fl} \left(D_{is} + 2(d_{os} + d_s) + d_{fl}\right) \pi \tag{23}$$

introducing eq. 23 in 22:

$$R_{DC} = \rho_{cu} \frac{N_{fl} \left(D_{is} + 2(d_{os} + d_s) + d_{fl}\right) \pi}{A_{fl-cond}} \tag{24}$$

The DC current is calculated as:

$$I_{fl} = J_{DC} A_{fl-cond} \tag{25}$$

Replacing eqs. 24 and 25 in 21, the conduction losses in the field winding can be calculated as:

$$P_{DC} = J_{DC}^2 \rho_{cu} \pi \left(D_{is} + 2(d_{os} + d_s) + d_{fl}\right) N_{fl} A_{fl-cond} \quad (26)$$

Using the definition of the field cooper factor K_{cu-fl}, this equation can be written as

$$P_{DC} = J_{DC}^2 \rho_{cu} \pi \left(D_{is} + 2(d_{os} + d_s) + d_{fl}\right) K_{cu-fl} A_{fl} \quad (27)$$

where ρ_{cu} is the copper resistivity.

2) AC losses: Similar to the DC losses, alternating current circulating along to the AC winding generate power losses given by:

$$P_{AC} = m_1 I_{AC}^2 R_{AC} \quad (28)$$

The AC resistance is calculated as:

$$R_{AC} = \rho_{cu} \frac{l_{coil}}{A_{ac-cond} C} \quad (29)$$

where C is the number of parallel circuits per phase, and l_{coil} is the average length the AC winding:

$$l_{coil} = 2\left(L_{st} + l_{head}\right) N_t \quad (30)$$

where l_{head} is the coil head length. Similar to the DC winding, the AC current is:

$$I_{AC} = J_{AC} A_{ac-cond} \quad (31)$$

therefore Joule losses due to the AC current are calculated as:

$$P_{AC} = m_1 J_{AC}^2 \rho_{cu} \frac{2\left(L_{st} + l_{end}\right)}{C} K_{cu-ac} A_{slot} \quad (32)$$

where, K_{cu-ac}

$$A_{slot} = \frac{N_t A_{ac-cond}}{K_{cu}} \quad (33)$$

B. Iron Losses

For the purpose of loss calculations, rotor losses have been neglected. Losses due to the time-varying flux are concentrated in the stator. Based on data provided by the manufacturer, the iron losses per kilogram, as a function of the flux density and frequency, can be approximated by the expression obtained by regression analysis. A close estimation is achieved with:

$$\frac{P_{iron}}{kilograms} = 0.001843 f^{1.4163} B^{(1.4427 + 0.0639 ln(f))} \quad (34)$$

Stator teeth and the laminated section of the stator core losses under time-varying flux, are estimated using previous equation.

Although, the solid portion of the stator core is not under time-variation magnetic flux, (PM and field flux are constant values), the rotor movement generates an alternating magnetic flux spatial variation. Similar to the DC machine armature, the relative movement of the rotor respect to the stationary flux results in a variable flux distribution. In the CPPM machine, magnets impose a constant magnitude of airgap flux, which close the circuit into the stator. As the rotor moves, the flux direction changes in the stator core as is shown in figure 7. As a result, iron losses are generated which are proportional to the speed.

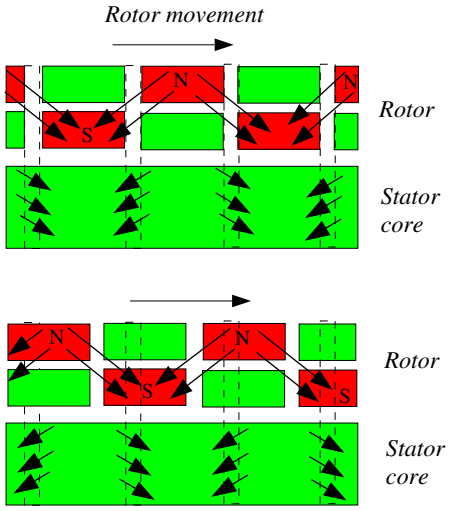

Fig. 7. Spatial flux variation in the stator core due to the rotor movement

Iron volumes of each section of the machine are given by the following expressions

* Stator teeth:

$$V_{th} = K_{st} t_s d_s S_1 \left[\left(l_{pm} + l_{iron}\right) + d_{os}(\pi D_{is} - w_{os} S_1)\right] \quad (35)$$

* Laminated stator core:

$$V_{lam} = K_{st} d_{fl} \pi (D_o - 2d_{cs} - d_{fl}) \quad (36)$$

* Solid stator core:

$$V_{sol} = d_{cs} \pi (D_o - d_{fl}) \quad (37)$$

Total mass of the iron is calculated as

$$H_{iron} = \gamma_{iron} V_{vol-iron} \quad (38)$$

where γ_{iron} is the iron density and its value correspond to $9.6 \times 10^6\ kg/m^3$

V. Field Ampere-Turns Requirement

Separating the total power generated by the machine according to how the excitation is originated. Two types of power are defined: P_{g-pm} represents the portion of the airgap power which is proportional to the PM magnetization: B_{g-pm}. According to the linear analysis model, the average airgap flux density in front of the PM is constant and is dependent on the magnet characteristics and airgap length (eq. 11). On the other hand, airgap flux density in front of the iron pole, B_{g-iron}, is proportional to the field Ampere-Turns, and the airgap length (eq. 5). The output power associated with this portion of the airgap flux density, P_{g-iron}, changes in accordance to the magnitude and direction of the field MMFs.

In order to determine the proportion of the power developed for each side of the airgap, different design constraints have to

be taken into account. The utilization level of the iron (mainly in the stator teeth and core), permanent magnet material and other geometric, magnetic, and technical considerations define the correct ratio between the power arising from the PM and field winding excitations. In general this power relationship can be expressed as:

$$K_{pw} = \frac{P_{g-iron}}{P_{g-pm}} \tag{39}$$

where K_{pw} is the Airgap Power ratio. This factor is defined for the maximum field AT condition. It can be easily shown that:

$$K_{pw} = \frac{B_{g-iron}}{B_{g-pm}} \tag{40}$$

therefore, solving for B_{g-iron}, and introducing this result in eq. 5

$$K_{pw} B_{g-pm} = \mu_o \frac{N_{fl} I_{fl}}{2g_e} \tag{41}$$

and solving for $N_{fl} I_{fl}$

$$N_{fl} I_{fl} = \frac{2g_e}{\mu_o} K_{pw} B_{g-pm} \tag{42}$$

Eq. 42 represents the amount of field Ampere-Turns necessary for a given value of power ratio and flux density in the PM section. The required amount of field ATs can be calculated for maximum magnetization (or demagnetizing) effect of the field winding. For excitations based on ferrite (lower remanence material), the major component of the airgap flux arises from the field excitation. This fact suggests that $K_{pw} > 1$. For a rare earth type of PM (such as NdFeB), this factor is close to unity. In order to maximize the use of the iron, similar maximum flux density values in both sides of the airgap must be selected. As a result, the associated power associated with each section of the airgap are similar. In terms of the airgap power ratio this consideration suggests: $K_{pw} = 1$.

VI. Flux Control Requirement

A. Motor Operation

From the phasor diagram and for the rated condition ($V_s = 1pu$, $I_s = 1pu$) and for unity power factor, the following expression can be derived:

$$E_f sin\delta = X_q cos^2\delta + X_d sin^2\delta \tag{43}$$

$$E_f cos\delta = 1 - \frac{(X_q - X_d)}{2} sin2\delta \tag{44}$$

Taking the quotient between these two equations, torque angle δ can be calculated as:

$$\delta = \arctan\left\{ \frac{(X_q - X_d)cos^2\delta + X_d}{1 - \frac{X_q - X_d}{2} sin(2\delta)} \right\} \tag{45}$$

It is clear that if the speed reaches the rated value (therefore current and voltage becomes 1 [pu]), the machine state is determined only by the *d-axis* and *q-axis* reactances. Using eq. 43 and 44, the expression for the back-emf can be calculated as:

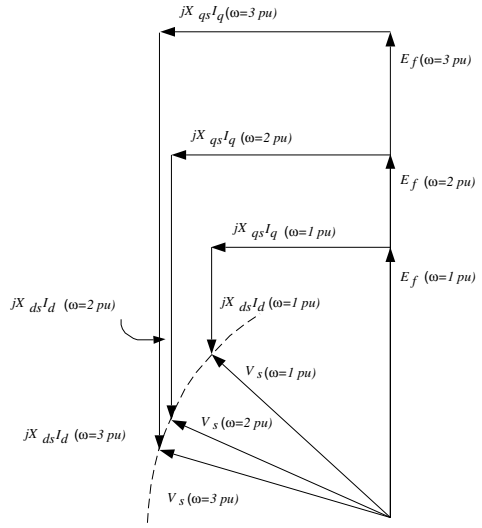

Fig. 8. Phasor diagram for constant power mode

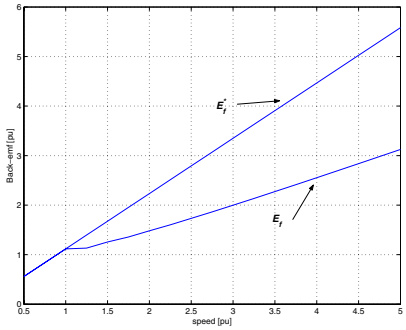

Fig. 9. Back-emf requirement to maintain unity terminals voltage as speed increases

$$E_f = \sqrt{\left[\Delta X cos^2\delta + X_d\right]^2 + \left[1 - \frac{\Delta X}{2} sin2\delta\right]^2} \tag{46}$$

where $\Delta X = X_q - X_d$

Clearly X_d and X_q vary with the speed and the torque angle changes according with eq. 45. Figure 8 shows a scaled phasor diagram for three different speeds in the constant power mode. As velocity increases, the amount of back-emf required does not increase in the same proportion, as the speed varies. Figure 9 depicts the variation of the back-emf as the velocity increases. In this picture E_f^* describes the variation of the back-emf if no weakening action is undertaken. As expected, this internal voltage increases linearly with the speed. eq. 45 is also plotted in the same figure, labeled as E_f. This equation represents the necessary back-emf to keep terminals voltage and current at rated values as the speed increases. The $y - axis$ difference between these two curves is the amount of field reduction that the field winding must provide. Clearly, the requirement for weakening action diminishes at high speed due to the values *d-axis* voltage drops. The $d - axis$ voltage drop has a demagnetizing

effect, and therefore the field weakening requirement is heavily influenced by the $d-axis$ reactance.

For motor operation, the magnetizing effect of the field flux is at its maximum at rated speed. Both sections of the airgap provide the excitation, and the field current is at its maximum. As the speed increases, this excitation must be reduced, reducing field current and eventually incrementing the field flux demagnetizing effect. According to figure 9, this variation is a non-linear function and is dependent on the machine parameters. Adequate selection of the 'non-field current' point must be done. This point corresponds only to the excitation produced by the PM (the field current is zero). Based on this condition, the number of AC winding turns can be calculated.

Ideally, maximum magnetizing (at rated speed) and demagnetizing (at maximum speed attainable) effects have to be reached with the same amount of DC field current. In this manner, DC field losses for both conditions are equalized.

B. Alternator Operation

Because generator operation requires the machine to supply power to an electrical load, the field flux control approach must be different compared to motor operation. Although terminal voltage control is the main goal current and power factor are variable which are determined by the load. This load can be considered as a constant power load, where the output voltage, current and power factor are constant for any speed operation. Other types of loads are variable impedance load, where current changes with the speed. Therefore, magnetizing and demagnetizing effects of the field flux must be called upon to compensate for these variations.

¿From the phasor diagram for the generating mode, the back-emf components can be written as:

$$E_f \sin\delta = I_s X_{dq} \cos(\phi) + \frac{I_s}{2}\sin(2\delta)\sin(\phi)\,[\Delta X] \quad (47)$$

$$E_f \cos\delta = V_s + I_s X_{qd} sin(\phi) + \frac{I_s}{2}\sin(2\delta)\cos(\phi)\,[\Delta X] \quad (49)$$

where:

$$X_{dq} = X_d \sin^2\delta + X_q \cos^2\delta \quad (50)$$

and

$$X_{qd} = X_q \sin^2\delta + X_d \cos^2\delta \quad (51)$$

The torque angle is calculated in the same manner as before. Utilizing these equations it is possible to calculate the required back-emf for any load condition as a function of the machine parameter and speed.

$$E_f = f(I_s, V_s, n_{pu}, X_{d_o}, X_{q_o})$$

where the subscript $'o'$ indicates a parameter calculated at some specific condition defined by the type of load supplied, current level, and power factor.

Constant Power Load: If output current and voltage are constants (for given power factor) over all ranges of speed, the field flux must compensate for the effect of speed variations. At low speed, PM excitation is not sufficient to maintain the required terminal voltage under heavy load, because of the low induced voltage (low speed). Extra flux must be provided by the field flux, such that the voltage is kept at a rated value. At high speed, excessive back-emf produced by the PM excitation must be reduced by the field flux weakening the airgap flux.

Balance between minimum and maximum speed DC field flux requirements must be considered in order to minimize conduction losses. Correct selection of the number of turns at the zero field current condition results in an adequate distribution of the DC field flux at low and high speed. The non-load current point depends upon the speed range, machine parameters and load power factor.

Constant Torque Load: Changes in the load, in terms of the magnitude and phase, impose similar type of constraints for the PM and field flux. Similar to the previous case, a particular DC field flux requirement depends on the selection of the operating point which defines the selection of the PM flux magnitude.

VII. Optimum DC field slot geometry

Because of the field winding location, the geometry of slot of the DC field must be calculated carefully. In fact, axial (d_{fl}) and radial (l_{fl}) DC slot lengths increment the total machine volume with no extra power gained. In addition the iron and PM length (l_{iron} and l_{pm}), axial length of the DC field slot increases the total stator length. A portion of the airgap associated with this length does not contribute to the energy conversion process due to the presence of zero airgap flux density in this region. As a result, overall power density becomes degraded as the axial length increases. The radial length also reduces the maximum power available for the machine. For a given value of AC slot depth and stator core, the radial length reduces the inner diameter (if the outer diameter is fixed) or increases the outer diameter (if the torque is keep constant). In the first case, torque is lower due to the smaller inner diameter. In the second case, the total volume increases. In either case power density is reduced. Consequently, selection of the DC field slot parameters has to be done to assure minimum volume of the machine.

Writing the expression for the total volume

$$vol = \frac{\pi}{4} D_{os}^2 L_{tot} \quad (52)$$

where the outer diameter is given by

$$D_{os} = D_{is} + 2(d_{os} + d_s + d_{fl} + d_{cs}) \quad (53)$$

and the total axial length of the machine is given by:

$$L_{tot} = l_{pm} + l_{fl} + l_{iron} + 2l_{end} \quad (54)$$

The area required to allocate the DC field winding can be computed as the product between the axial and the radial lengths

$$A_{fl} = d_{fl} l_{fl} \quad (55)$$

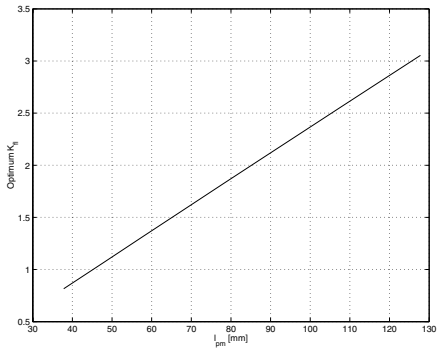

Fig. 10. Optimum K_{fl} for different total lengths of the machine $L_{tot} = l_{pm} + l_{iron} + l_{fl} + 2l_{end}$

Defining K_{fl} as the ratio between these two variables

$$K_{fl} = \frac{l_{fl}}{d_{fl}} \tag{56}$$

Then the radial length can be expressed as:

$$d_{fl} = \sqrt{\frac{A_{fl}}{K_{fl}}} \tag{57}$$

and the axial length

$$l_{fl} = \sqrt{K_{fl} A_{fl}} \tag{58}$$

Introducing eqs. 57 and 58 in eqs. 53 and 54, and the in eq. 52, the expression for the total volume of the machine is obtained. The resultant expression is a quadratic equation in term of K_{fl}. Knowing the AC slot geometry, the total DC field slot area, and the PM and iron pole axial length, the optimum value for the DC slot aspect ratio is found. The final expression for this parameter is:

$$K_{fl} = \left[\frac{\sqrt{A_{fl}} + \sqrt{A_{fl} + 4D_{os}(l_{pm} + l_{iron} + 2l_{end})}}{D_{os}} \right]^2 \tag{59}$$

Using 59 and eqs. 57 and 58 the outer diameter of the machine can be calculated.

Figure 10 shows how the optimum value of K_{fl} changes when the length of the machine increases.

VIII. AC Slot geometry including DC Slot Geometry

In previous work [1], the AC slot parameters were calculated in order to maximize airgap power under the current loading constraint. However, DC field slots alter this optimum geometry, increasing the axial length and also modifying the diameter ratio. Therefore, a redesign of the AC Slot geometry has to be done, in order to match the surface current density restriction.

Writing the current loading [5], for the condition where the DC winding is not considered

$$A_{s1} = \frac{K_{cu} A_{slot1} S_1}{\pi D_{is1}} J_{rms1} \tag{60}$$

where A_{slot1} and D_{is1} are the slot area and inner stator diameter obtained from the AC slot geometry optimization.

Inclusion of the slot to allocate field winding reduces the inner diameter as well as the AC slot area. Writing the expression for the surface current density for this second condition:

$$A_{s2} = \frac{K_{cu} A_{slot2} S_1}{\pi D_{is2}} J_{rms2} + \frac{K_{cu} A_{fl}}{\pi D_{is2}} J_{fl} \tag{61}$$

The second right-hand component of eq. 61, correspond to the additional current loading due to the field winding. In order to have the same cooling capabilities in both cases, both current loadings must be equal

$$A_{s1} = A_{s2} \tag{62}$$

Replacing eqs. 60 and 61 in eq. 62, this equality becomes

$$\frac{A_{slot1} S_1}{D_{is1}} J_{rms1} = \frac{A_{slot2} S_1}{D_{is2}} J_{rms2} + \frac{A_{fl}}{D_{is2}} J_{fl} \tag{63}$$

assuming equal AC and DC current densities, the condition for equal current loading is reached if the inner diameter is:

$$D_{is2} = \frac{A_{slot2} S_1 + A_{fl}}{A_{slot1} S_1} D_{is1} \tag{64}$$

Eq. 64 establishes that stator inner diameter is smaller in proportion after considering the field winding and the DC slot area. Reduction of the inner diameter implies an output torque reduction for a given airgap flux and current density. In addition, a larger stator core, proportional to the radial dimension of the DC slot, increases material, weight and ultimately iron losses. These are the inevitable trade-offs using the field winding to obtain airgap flux control capabilities. However, speed range extension (motor operation) and wide range of the terminal voltage control(generator operation) are the corresponding benefits.

IX. Design Flow Diagram

Based on equations and design criteria developed in the previous sections, a general procedure to design a CPPM machine is presented. Figures 11 and 12 depict the sequence of steps to be followed to obtain a desired machine performance.

For given design parameters such as: power output, flux density distribution (airgap, teeth, core), airgap flux variation range, etc; the design procedure begins with stator diameters calculation and AC winding slot parameters. With flux density, external aspect ratio, current density and electric current loading values, for each portion of the magnetic circuit, an optimum stator diameter ratio is calculated to achieve maximum airgap power. Using that result, AC stator slot and core dimensions are computed.

The next step is to compute the DC field slot area. With the airgap power ratio, flux density at the PM section, and DC current density, the area required for the field winding to overcome the airgap length is found. Optimum dimension (axial and radial lengths) of this slot are calculated to minimize the total machine volume. This slot area is defined by the amount of field MMF calculated in accordance with airgap power ratio.

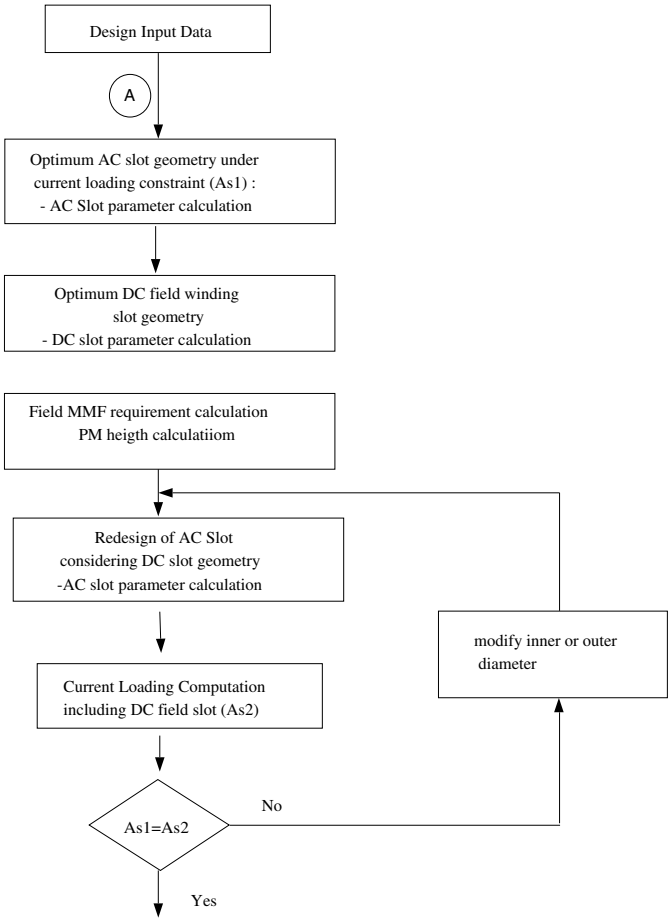

Fig. 11. Design flow diagram for the CPPM machine

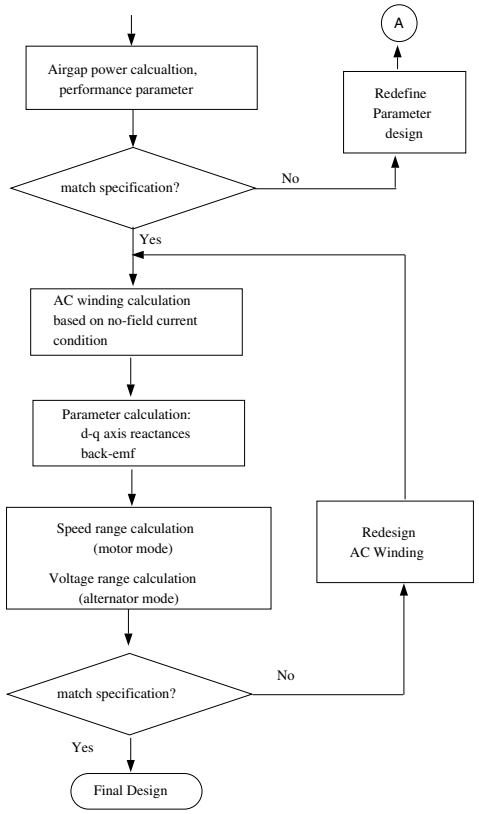

Fig. 12. Design flow diagram for the CPPM machine (continuation)

The extra space occupied by the DC slot requires that a new diameter ratio be calculated, in order to keep the same electrical current loading. At this point a decision must be taken. Adjustment of the inner and/or outer diameters have to be made to maintain the flux density distribution at the predefined level. With new diameters, a re-computation of the AC stator slot parameter is done up to match the cooling constraint.

After this stator design procedure, output power and performance parameters are calculated. If any of this numbers do not match with the specification, a stator redesign must made. Inner or outer (depending on the design constraint) diameters and external aspect ratios are adjusted to initiate the procedure again.

The next step is to design the AC winding according to the application. Based on zero-field current (only PM excitation of the machine); the number of turns are calculated. Then $dq-axis$ reactances are computed in accordance with the geometry of the rotor parameters. For motor operation, maximum torque (for constant V/Hz region) and speed range (for constant power region) are determined. Associated field losses are also estimated. For alternator operation, the load type and, flux requirements to keep a constant terminal voltage can be evaluated. If the speed range or regulation condition are not matched, a redesign of the AC winding must be made by selecting a different speed to calculate the AC winding turns number for the no-field current condition.

X. Conclusion

In this paper a simplified reluctance equivalent circuit for the CPPM machine for design purposes is derived. This circuit allows us to determine the airgap flux and the airgap flux density considering both: PM and field winding excitation.Also, expressions for the AC winding slot and DC field slot geometries can be derived. Copper and iron losses are computed based on manufacturer material data. Particular attention is made to calculate iron losses in the stator yoke where the flux fluctuates due to the rotor speed. The accuracy of the approached is confirmed by comparison with a 3D-FE solution. An optimization process is outlined to maximize the material utilization under current and magnetic loading constraints. Finally a flow diagram is presented to guide the design process.

References

[1] J.A. Tapia, F. Leonardi, T.A. Lipo, "Consequent Pole Permanent Magnet Machine With Field Weakening Capability," IEEE International Electric Machines and Drives Conference, IEMDC 2001. Cambridge MA, pp. 126-131.

[2] V.Ostovic, J.M. Miller, V.K Gark, R.D.Schultz, S.H.Swales, "A Magnetic-Equivalent-Circuit-Based Performance Computation of a Lundell Alternator," IEEE T-IA, Vol. 35,No. 4,July/August 1999, pp. 825-830.

[3] Runghai Qu, " Design and Analysis of Dual-Rotor, Radial-Flux, Toroidally-Wound, Surface-Mounted-PM Machine," Ph.D. Thesis. University of Wisconsin-Madison. May 2001.

[4] D. C. Hanselmann, "Brushless Permanent-Magnet Motor Design," McGraw-Hill, 1994.

[5] T.A. Lipo *Introduction to AC Machine Design* Classroom text for course ECE 713, University of Wisconsin-Madison, 1995.